

# Capillary fluctuations in non-equilibrium systems

James E. McClure

*Virginia Polytechnic Institute & State University, Blacksburg*

Steffen Berg

*Shell Global Solutions International B.V. Grasweg 31, 1031HW Amsterdam, The Netherlands*

Ryan T. Armstrong

*University of New South Wales, Sydney*

(Dated: December 27, 2022)

We develop non-equilibrium theory to account for non-ergodic effects that arise due to macroscopically “slow” fluctuations in heterogeneous systems. The derived theory is broadly applicable to describe athermal fluctuations, particularly those that do not obey detailed balance. An area of application are fluctuations in capillary-dominated systems, which are non-stationary due to the irreversibility of cooperative events. Considering droplet coalescence alongside capillary fluctuations that occur for immiscible fluid displacement in porous media, we show that a simple power law is insufficient to predict the spectral power density  $S_P$  for capillary fluctuations. Instead, we find that  $S_P$  is linked to frequency  $F$  based on an exponential relationship,  $\log S_P \sim \alpha F^p$ , with  $\alpha = -15$  and  $p = 1/2$  describing the fluctuations of both systems.

The ergodic hypothesis is central to many results of statistical physics. The basic premise is that a system will explore all possible energetic micro-states if considered over a sufficiently long interval of time. The concept of ergodicity is thereby linked with the mixing of information within a system [1]. Canonical proofs of the ergodic hypothesis rely on the equivalence of spatial and temporal averages in the limit of infinite time [2, 3]. Scale considerations and the rate of mixing necessarily constrain the applicability of the ergodic hypothesis when considering finite regions of time, particularly for systems where mixing is slow compared to the physical timescale of interest [4]. Many physical systems are known to exhibit behavior that is inconsistent with the ergodic hypothesis. Well known examples include anomalous diffusion in biological systems [5–7], glassy systems [8–10], capillary phenomena and nucleation [11–16] and granular systems where multiscale effects are present due to jamming and force chains [17–20]. A common element for these systems is that they involve spatially heterogeneous materials where available thermal energy is insufficient to overcome internal energy barriers. This inhibits mixing and prevents the system from exploring all possible micro-states within the timescale of interest. In this paper, we demonstrate that time-and-space averaging can be applied as a mechanism to mathematically mix information at the desired scale, providing a natural path forward in systems where non-ergodic effects are encountered. Multiscale fluctuation terms arise in the non-equilibrium description due to spatial and temporal deviations associated with intensive thermodynamic variables. Our approach is rooted in classical thermodynamics and offers a formally distinct perspective on fluctuations as compared to statistical theory, e.g. [21–25]. The approach will be applied to non-equilibrium behavior

in multiphase systems, where fluctuations occur due to capillary effects and confinement. How to characterize and interpret these fluctuations has been a long-standing problem for immiscible fluid flow in porous media, and has broad applications to other systems [28–37].

A classical thermodynamic description is defined by considering the internal energy to depend on the entropy  $S$  as well as other extensive physical properties of the system,  $X_i$  (e.g. volume, number of particles, etc.) [38]

$$U = U(S, X_1, X_2, \dots, X_n). \quad (1)$$

Intensive quantities are then defined according to Euler’s homogeneous function theorem,

$$T = \left( \frac{\partial U}{\partial S} \right)_{X_i}, \quad Y_i = \left( \frac{\partial U}{\partial X_i} \right)_{S, X_{j \neq i}}, \quad (2)$$

such that

$$U = TS + X_i Y_i \quad (3)$$

describes the internal energy of the system at equilibrium. In practice, measurements of thermodynamic quantities are averages carried out over some finite region of space and time. If  $\mathcal{V}$  is the volume associated with a thermodynamic measurement, the measurement time can be chosen such that local equilibrium conditions apply at that scale. For example, if a thermometer is used to measure the temperature,  $\mathcal{V}$  is the volume of the measurement region that can be considered as being in local equilibrium with the measured value. We wish to develop theory that holds over some arbitrarily larger spatial region  $\Omega$  and time interval  $\Lambda$ , which has duration  $\lambda$ . To define larger scale measures we apply the time-and-space averaging operator

$$\langle f \rangle \equiv \frac{1}{\lambda \mathcal{V}} \int_{\Lambda} \int_{\Omega} f dV dt. \quad (4)$$

Averages are defined such that extensive quantities retain the same physical meaning,

$$\bar{U} \equiv \langle U \rangle, \quad \bar{S} \equiv \langle S \rangle, \quad \bar{X}_i \equiv \langle X_i \rangle. \quad (5)$$

The intensive quantities are then defined as [39]

$$\bar{T} \equiv \frac{\langle TS \rangle}{\langle S \rangle}, \quad \bar{Y}_i \equiv \frac{\langle X_i Y_i \rangle}{\langle X_i \rangle}. \quad (6)$$

These definitions ensure that the representation of the system energy is scale-consistent, e.g., the product of entropy and temperature corresponds to the thermal energy. Since entropy is additive, the temperature should be defined as the average thermal energy per unit of entropy. The averaged form is thus consistent with Eq. 3,

$$\bar{U} = \bar{T}\bar{S} + \bar{X}_i\bar{Y}_i. \quad (7)$$

Non-equilibrium behavior can be considered by averaging the differential form of Eq. 3

$$\begin{aligned} \frac{\partial \bar{U}}{\partial t} &= \left\langle T \frac{\partial S}{\partial t} \right\rangle + \left\langle Y_i \frac{\partial X_i}{\partial t} \right\rangle \\ &= \bar{T} \frac{\partial \bar{S}}{\partial t} + \left\langle (T - \bar{T}) \frac{\partial S}{\partial t} \right\rangle \\ &\quad + \bar{Y}_i \frac{\partial \bar{X}_i}{\partial t} + \left\langle (Y_i - \bar{Y}_i) \frac{\partial X_i}{\partial t} \right\rangle, \end{aligned} \quad (8)$$

We now define multiscale deviation terms as

$$T' \equiv T - \bar{T}, \quad Y'_i \equiv Y_i - \bar{Y}_i. \quad (9)$$

Using the definitions from Eqs. 5 and 6 we can show that

$$\left\langle T' \frac{\partial S}{\partial t} \right\rangle = - \left\langle S \frac{\partial T'}{\partial t} \right\rangle, \quad \left\langle Y'_i \frac{\partial X_i}{\partial t} \right\rangle = - \left\langle X_i \frac{\partial Y'_i}{\partial t} \right\rangle. \quad (10)$$

which can be substituted into Eq. 8 and rearranged to obtain an entropy inequality

$$\frac{\partial \bar{S}}{\partial t} = \frac{1}{\bar{T}} \left[ \frac{\partial \bar{U}}{\partial t} - \bar{Y}_i \frac{\partial \bar{X}_i}{\partial t} + \underbrace{\left\langle S \frac{\partial T'}{\partial t} \right\rangle + \left\langle X_i \frac{\partial Y'_i}{\partial t} \right\rangle}_{\text{fluctuation terms}} \right] \geq 0. \quad (11)$$

The result is easily recognizable as the fundamental relation of non-equilibrium thermodynamics (e.g. [40]), but with additional terms associated with fluctuations. The fluctuations contribute to the energy dynamics whenever intensive variables deviate from their average values within the spatial region  $\Omega$  and time interval  $\Lambda$ . In other words, these terms are linked with multiscale effects associated with processes that occur at a length scale smaller than  $\Omega$  or based on time scale smaller than  $\Lambda$ .

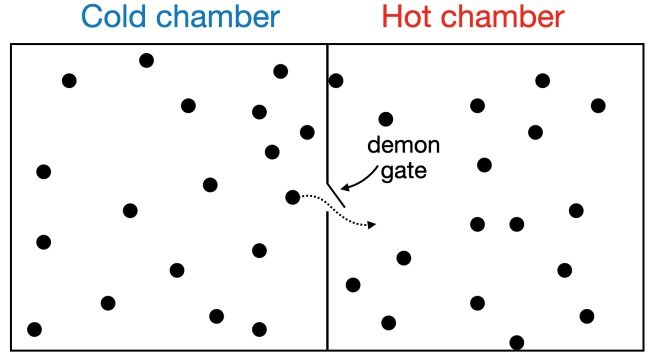


FIG. 1. “Maxwell’s demon” considers a thought experiment in which a demon selectively permits the migration of hot molecules from one chamber to the other. Due to the heat flux carried by the transmitted molecules, the temperature of the hot chamber increases, leading to a thermal gradient between the chambers. The demon’s actions are constrained by a symmetry law relating thermal fluctuations.

### Maxwell’s demon

To illustrate the role of fluctuations in non-equilibrium systems, we consider the actions of Maxwell’s demon [41, 42]. The traditional example is defined in terms of the two-chamber system shown in Figure 1. The demon operates a gate between two chambers, selectively allowing fast-moving molecules to move from the cold chamber to the hot chamber. In apparent violation of thermodynamic intuition, the associated heat flux increases the temperature of the hot chamber. Maxwell’s demon can be considered in the context of non-ergodic behavior, as the demon controls the mixing of information between the two chambers. In our analysis, we assume that for each “hot” particle that moves from left to right, the demon allows a “cold” particle to move from right to left so that the particle density within the chamber remains unchanged. This allows us to ignore the fluctuation of the particle density. Actions of the demon are a non-equilibrium behavior, since there is a heat flux associated with the kinetic energy of the transmitted particles. The system is spatially heterogeneous, and the chambers can be denoted as two sub-sets of the system,  $\Omega_h$  and  $\Omega_c$ . Based on these definitions a discrete aspect is introduced into the representation of the system, since the crossing of molecules from one sub-domain to the other occur as discrete events. Time averaging will smooth out the effect of these crossings such that the action of the demon can be modeled as being continuous with respect to time.

The temperature and entropy are spatially segregated by defining separate fields for each chamber

$$T_i \equiv T \Upsilon_i, \quad S_i \equiv S \Upsilon_i, \quad (12)$$

where the indicator function  $\Upsilon_i$  identifies the region

$$\Upsilon_i(\mathbf{x}) = \begin{cases} 1 & \text{if } \mathbf{x} \in \Omega_i \\ 0 & \text{otherwise} \end{cases} \quad (13)$$

for  $i \in \{h, c\}$ . Consistent with Eqs. 5 and 6, we now define the temperature and entropy within each chamber

$$\bar{S}_i \equiv \langle S_i \rangle, \quad \bar{T}_i \equiv \frac{\langle T_i S_i \rangle}{\langle S_i \rangle}. \quad (14)$$

These definitions ensure that the entropy is additive,

$$\bar{S} = \bar{S}_c + \bar{S}_h, \quad (15)$$

and that the total thermal energy is conserved based on the definition of the temperature,

$$\bar{T}\bar{S} = \bar{T}_c\bar{S}_c + \bar{T}_h\bar{S}_h. \quad (16)$$

The thermal fluctuation terms in Eq. 11 impose a symmetry constraint on the demon's action. Because the two-chamber system is closed, the total internal energy does not change. Since the demon is part of the closed system, this is true even if the demon dissipates energy, as dissipated energy will simply go directly back to thermal energy. We assume only that the demon is passive in the sense that it does not store energy. Omitting the extensive measures  $X_i$ , the thermal effects must obey

$$\bar{T} \frac{\partial \bar{S}}{\partial t} - \left\langle S \frac{\partial T'}{\partial t} \right\rangle = 0. \quad (17)$$

From statistical arguments it is clear that the demon does not alter the global entropy. The probability to find a molecule with a particular kinetic energy does not change based on the crossing event. The demon merely segregates the spatial arrangement of particles. The global rate of entropy production is therefore zero, implying that the process is reversible. The remaining term is due to the temperature fluctuation within the system. This can be sub-divided to obtain a relationship between the fluctuations in each chamber,

$$\left\langle S_c \frac{\partial T'_c}{\partial t} \right\rangle + \left\langle S_h \frac{\partial T'_h}{\partial t} \right\rangle = 0 \quad (18)$$

where  $T'_i = T_i - \bar{T}$  on  $\Omega_i$ . This establishes a thermodynamic symmetry law for the reversible heat flux between the two chambers,

$$\frac{\partial Q}{\partial t} = \left\langle S_h \frac{\partial T'_h}{\partial t} \right\rangle = - \left\langle S_c \frac{\partial T'_c}{\partial t} \right\rangle. \quad (19)$$

The symmetry stated in Eq. 19 may be broken for athermal fluctuations in systems that dissipate energy, or when other terms contribute to the energy dynamics. Eq. 19 is a simple statement that thermal fluctuations must obey conservation of energy, identical to the result established

from the perspective of microscopic reversibility[47, 48]. The key step in establishing the result from classical thermodynamics is the scale-consistent definition of temperature and entropy. The result is a simple fluctuation theorem that does not require *information*, as has been proposed in many other treatments of this problem [43–46]. Since thermodynamics express conservation of energy, one simply needs to ensure that definitions of thermodynamic quantities account for all energy in the system. For this reason it is essential that averaged thermodynamics maintain scale consistency. More generally, the demon illustrates two important features of systems where multi-scale fluctuations are important. First, it defines an energy barrier that prevents mixing between the hot and cold chambers. Second, the problem is associated with gradients in an intensive thermodynamic property. We now demonstrate the importance of these terms in capillary-dominated systems, where gradients in composition and chemical potential lead to length scale heterogeneity. The dependence of the system energy on the interface configuration causes cooperative behavior when the interfaces are disrupted. These transient effects are captured based on multiscale fluctuations.

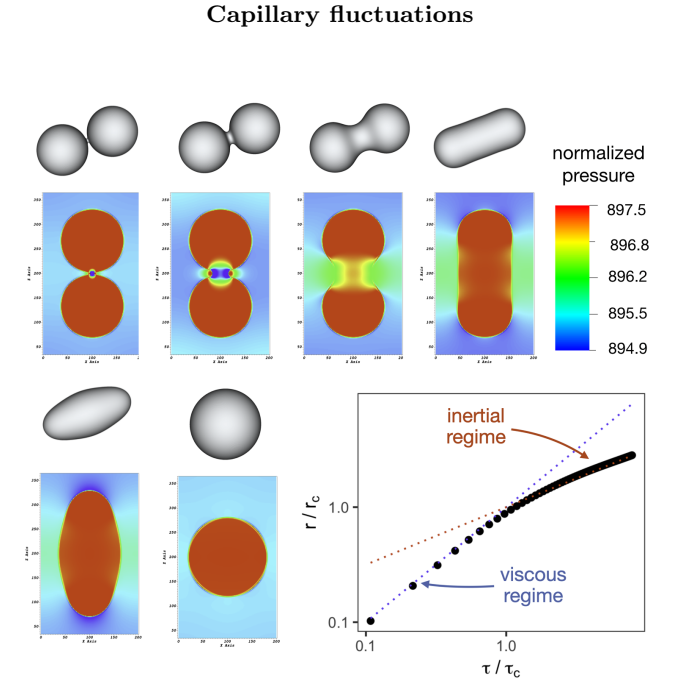


FIG. 2. Droplet coalescence leads to fluctuations in the pressure field (color) due to the rapid change in capillary forces. Scaling for the coalescence event is limited by viscous forces during the initial bridge formation, and is dominated by inertial forces at late times.

The coalescence of two fluid droplets represents one the simplest examples of topological change in fluid mechanics. The topological event induces an apparent singular-

ity at the point of coalescence, which is then followed by a cascade of energy dissipation that is governed by distinct scaling regimes as the system establishes a new equilibrium. At equilibrium, the fluid pressures and interface curvature are related based on the Young-Laplace equation

$$p_n - p_w = \gamma_{wn} \left( \frac{1}{R_1} + \frac{1}{R_2} \right), \quad (20)$$

where  $R_1$  and  $R_2$  are the principal curvatures along the interface between fluids and  $\gamma_{wn}$  is the interfacial tension. Detailed studies of the droplet coalescence mechanism show that the flow behavior and associated geometric evolution are coupled on a very fast timescale [49–56]. At the molecular level, coalescence is initiated based on thermal effects [57]. Hydrodynamic effects become dominant after approximately 30 picoseconds, based on the formation of a bridge that joins the droplets. The ensuing dynamics can be separated into two distinct regimes [55]. At early times, viscous effects dominate and the growth of the bridge radius scales as

$$\frac{r}{r_c} \sim \frac{\tau}{\tau_c}, \quad (21)$$

where  $\tau_c$  is the crossover time and  $r_c$  is the associated length scale. At late times, inertial effects dominate and the growth of the bridge radius scales as

$$\frac{r}{r_c} \sim \sqrt{\frac{\tau}{\tau_c}}. \quad (22)$$

Analogous results have been obtained for droplet snap-off [37]. The sequence depicted in Fig. 2 shows the effect of the coalescence event on the fluid pressure field as simulated by a lattice Boltzmann model [58]. The droplet volume was chosen so that the final radius for the simulation was  $R_f = 80$  voxels. Results demonstrate that simulation accurately recovers the predicted scaling behavior. In Fig. 2 the pressure field is normalized based on the interfacial tension and the final droplet radius,  $p_i^* = p_i R_f / \gamma_{wn}$ . The non-equilibrium behaviour for the pressure field develops as a response to the near instantaneous curvature disruption along the fluid-fluid interface at the point where the droplets first touch. The associated pressure shock drives the ensuing dynamics, dominated by fluctuations generated by the interfacial rearrangement. Capillary fluctuations are distinct from thermal fluctuations due to the fact that they are inherently cooperative in nature, and are linked to both reversible and irreversible energy transfer. The behavior is non-ergodic because capillary energy barriers inhibit the mixing of information between the droplets prior to the event; energy micro-states associated with the final droplet configuration are not explored before coalescence. Rapid mixing occurs after coalescence, once the energy barrier separating the two droplets has been destroyed.

To describe the thermodynamics of the system, we consider Eq. 2 in the form

$$U = U(S, V_w, V_n, A_{wn}), \quad (23)$$

where  $V_w$  and  $V_n$  are the volume of the droplet and the surrounding fluid and  $A_{wn}$  is the interfacial area between fluids. The associated intensive variables are the pressures  $p_w$  and  $p_n$  and the interfacial tension  $\gamma_{wn}$ . Averaging in time and space and assuming: (1) isothermal conditions; (2) constant interfacial tension; (3) the volume of each fluid is constant; and (4) compositional effects are negligible, Eq. 11 then simplifies to

$$\frac{\partial \bar{S}}{\partial t} = -\frac{1}{T} \left[ \left\langle V_w \frac{\partial p'_w}{\partial t} \right\rangle + \left\langle V_n \frac{\partial p'_n}{\partial t} \right\rangle + \bar{\gamma}_{wn} \frac{\partial \bar{A}_{wn}}{\partial t} \right] \geq 0. \quad (24)$$

Dissipative effects are understood by considering the fluctuation of the fluid pressures that are induced by the spontaneous change in surface energy. Comparing to Eq. 19, we see that energy conservation no longer implies the symmetry of the pressure fluctuation due to contributions from rate of change in surface energy and the fact that energy is dissipated. In our analysis, the full system is used as the domain for spatial averaging and the time interval is  $\Lambda = 0.108\tau_c$ , corresponding to 100 timesteps in the simulation.

Thermal fluctuations due to molecular effects are usually assumed to be stationary with respect to time as a consequence of the time reversibility of the Hamiltonian at the molecular level [22]. Capillary events are cooperative in nature and do not obey detailed balance due to the fact that energy is dissipated. The associated fluctuations are non-stationary because the equilibrium pressure values before coalescence differ from those in the final configuration. Symmetry-breaking is a consequence of the structural rearrangement associated with the transition to a new local minimum energy configuration. For a closed system the dissipated energy is easily calculated from the initial and final configurations, since at equilibrium the droplets are spherical. The energy dissipated is computed from the associated energy difference. Subject to the assumptions listed above, the entropy change is

$$\Delta S = \frac{1}{T} (V_w \Delta p_w + V_n \Delta p_n - \gamma_{wn} \Delta A_{wn}), \quad (25)$$

The radius for the initial and final droplets can be computed analytically based on the volume, making use of the Young-Laplace equation to determine the equilibrium fluid pressures.

The rate of energy change associated with capillary fluctuations is shown in Fig. 3. The timescale is normalized by the crossover time,  $\tau_c$ , which can be considered as defining the intrinsic timescale for the coalescence event. Immediately after coalescence, surface energy performs local work against the fluid pressure due to unbalanced capillary forces in the vicinity of the coalescence point.

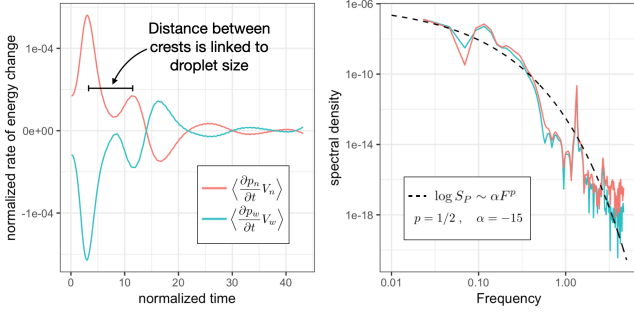


FIG. 3. Pressure fluctuation during energy redistribution resulting from the coalescence of two fluid droplets. (A) rate of energy change associated with pressure fluctuation relative to the final surface energy during droplet coalescence event; and (B) noise spectrum associated with capillary fluctuations can be predicted by  $\log S_P \sim \alpha F^p$ .

In this context, the pressure fluctuation terms are understood as resulting from local gradients in the pressure field that are generated due to the curvature discontinuity. These gradients are clearly visible in Fig. 2. Since the initial and final droplet states have different capillary pressure, the pressure fluctuation is not stationary over the event. Nevertheless, a large degree of symmetry is clear based on the mirroring effect between the pressure fluctuation in one fluid and the other. This suggests that the choice to represent the system in a discrete way introduces asymmetry into the system description. The Gibb's dividing surface defines a set operation that sub-divides the system into distinct geometric regions for each fluid, each with its own pressure. While topological changes such as droplet coalescence are fundamentally discrete events when considered from the perspective of set theory, set construction is a choice imposed on the system, as opposed to an underlying property of the physical system itself. Set operations are the basis for separately defining  $p_w$  and  $p_n$ . Detailed balance is not obeyed when the fluids are considered separately, since irreversible energy exchanges occur between the fluids due to cooperative rearrangement of the interface. For this reason symmetry is a property of the global system and not a property of the sub-regions.

Pressure fluctuations are multiscale rate effects that arise due to spatial heterogeneity in the potential field. The length scale associated with the heterogeneity is the driving factor that determines the spectral properties. Due to length scale effects the noise signature associated with capillary fluctuations is distinct from pink noise, where the relationship between the spectral density  $S_P$  and frequency  $F$  is  $S_P \sim 1/F$  [59–61]. A simple power law is insufficient to describe noise due to capillary fluctuations. Instead, we find that the scaling relationship is exponential,

$$\log S_P \sim \alpha F^p. \quad (26)$$

The coefficients  $\alpha$  and  $p$  are associated with the rate of decay in the spectral density as the frequency increases.  $S_P$  decays rapidly with  $F$  for frequencies that are faster than a typical event. For droplet coalescence  $\alpha = -15$  and  $p = 1/2$  match well with the simulated fluctuation spectrum.

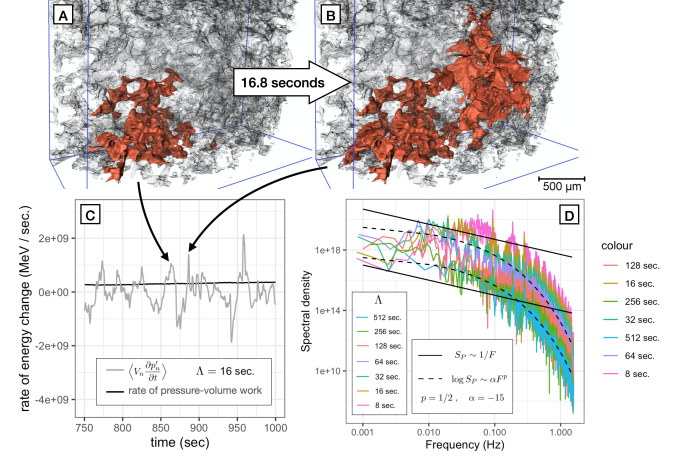


FIG. 4. Capillary fluctuations during displacement in porous media are linked with spontaneous pore-scale events that occur due to capillary forces within the solid micro-structure. Haines jumps occur spontaneously during immiscible displacement as the system “jumps” from (A) one energy minimum to (B) the next; (C) fluid pressure fluctuations arise due to these dynamics; and (D) scaling behavior for the power spectrum is independent of the time averaging interval.

The scaling relationship given by Eq. 26 also holds for much more complicated immiscible displacements in porous media. Cooperative events occur routinely as fluids migrate through complex micro-structure under the influence of capillary forces. Experimental data demonstrates that the timescale for these events is directly linked to the frequency for fluctuations in the pressure signal. Results shown in Fig. 4 were obtained using synchrotron micro-tomography imaging for flow of oil and brine in Berea sandstone. The system was initially saturated with brine, and oil was injected into the sample at a rate of  $0.35 \mu\text{L}/\text{minute}$ . Pressure transducer measurements were collected at an interval  $\Delta t = 0.32$  sec. For complete experimental details the reader is referred to Berg et al. [28]. Initial and final states for a pore-scale event known as a Haines jump are shown in Fig. 4A and 4B. Haines jumps are spontaneous events that occur when the fluid meniscus passes through narrow pore throats within the solid micro-structure, where the capillary pressure is high. As fluid spontaneously flows into the adjacent pore body, the capillary pressure drops rapidly causing a fluctuation in the signal [31]. The energy associated with the fluctuations is relatively large as compared to rate of pressure-volume work (see Fig. 4C). The timescale for pore-scale events is controlled by the solid micro-structure, which means that the statistics

for the associated noise signal are linked to length scale heterogeneity within the system. In spite of this considerable complexity, the scaling behavior is predicted from Eq. 26 with identical coefficients to the droplet coalescence problem. Averaging over a longer time interval reduces the amplitude of the fluctuations due to cancellation of positive and negative parts, but does not change  $\alpha$  and  $p$ . Due to the energy dissipated during cooperative events, the distribution for the fluctuations can be asymmetric, meaning that the mean value of the fluctuation is not zero. For the data shown in Fig. 4 the net contribution from fluctuations is 7.84% of the total pressure-volume work when considered over  $\Lambda = 512$  seconds. The implication is that even when local equilibrium conditions apply at a microscopic length scale, they do not necessarily hold for larger length scales. In this situation fluctuation terms must be included explicitly in the non-equilibrium thermodynamics, since these terms are needed to state conservation energy for the system.

### Conclusions

We derive non-equilibrium thermodynamic expressions using time-and-space averaging, showing that fluctuations for intensive variables arise due to multiscale heterogeneity. Fluctuations are linked with sub-scale gradients for intensive thermodynamic quantities, which have a tendency to relax toward equilibrium at a macroscopically slow timescale determined based on the length scale associated with the gradients. In contrast with thermal fluctuations, multiscale fluctuations are linked with cooperative events and therefore may not obey detailed balance. This can cause the fluctuations to be non-stationary. As an example we consider capillary fluctuations due to droplet coalescence and immiscible displacement in porous media. We show that capillary fluctuations can be predicted by a simple scaling law,  $\log S_P \sim \alpha F^p$ , with  $\alpha = -15$  and  $p = 1/2$  matching the fluctuation spectrum in both cases. Multiscale fluctuations are extensible to other systems where gradients in composition, chemical potential, and other intensive variables are operative at a scale smaller than the scale of interest. Classes of non-ergodic behavior that are defined by macroscopically slow physics are particularly relevant.

### Acknowledgements

‘An award of computer time was provided by the Department of Energy Summit Early Science program. This research also used resources of the Oak Ridge Leadership Computing Facility, which is a DOE Office of Science User Facility supported under Contract DE-AC05-00OR22725.  $\mu$ CT was performed on the TOMCAT beamline at the Swiss Light Source, Paul Scherrer Insti-

tut, Villigen, Switzerland. We are grateful to G. Mikuljan at Swiss Light Source, whose outstanding efforts have made these experiments possible’

- 
- [1] W. Parry, *Topics in Ergodic Theory*. Cambridge Tracts in Mathematics. Cambridge University Press, 2004.
  - [2] J. v. Neumann, Proc. Natl. Acad. Sci. U.S.A. **18** 70 (1932).
  - [3] G. D. Birkhoff, Proc. Natl. Acad. Sci. U.S.A. **17**, 656 (1931).
  - [4] R.G. Palmer, Adv. Phys. **31**, 669 (1982).
  - [5] A V. Weigel, B. Simon, M. M. Tamkun and D. Krapf, Proc. Natl. Acad. Sci. U.S.A. **108**, 6438, 2011.
  - [6] M. Schwarzl, A. Godec and R. Metzler, Sci. Reports, **7**, 3878 (2017).
  - [7] F. S. Gnesotto, F. Mura, J. Gladrow and C. P. Broedersz, Reports Prog. Phys., **81**, 066601 (2018).
  - [8] P. G. Debenedetti and F. H. Stillinger, Nature, **410**, 159 (2001).
  - [9] A. Crisanti and F. Ritort, J. Phys. A: Math. Gen. **36**, R181 (2003).
  - [10] G. Tarjus, S. A. Kivelson, Z. Nussinov and P. Viot, J. Phys. Cond. Matter, **17**, R1143 (2005).
  - [11] S.S. Datta, H. Chiang, T. S. Ramakrishnan and D. A. Weitz, Phys. Rev. Lett., **111**, 064501, (2013).
  - [12] V. D. Bormann, A. A. Belogorlov, V. A. Byrkin and V. N. Tronin, Phys. Rev. E, **88**, 052116, (2013).
  - [13] D. Crandall, G. Ahmadi, M. Ferer and D. H. Smith, Physica A: Stat. Mech. App., **388**, 574 (2009).
  - [14] E. Kierlik, P. A. Monson, M. L. Rosinberg, L. Sarkisov and G. Tarjus, Phys. Rev. Lett., **87** 055701 (2001).
  - [15] M. Winkler, M. Gjennestad, D. Bedeaux, S. Kjelstrup, R. Cabriolu and A. Hansen, Frontiers Phys., **8**, 60 (2020).
  - [16] M. Iwamatsu, J. Chem. Phys. **134** 164508 (2011).
  - [17] A. Baule, F. Morone, H. J. Herrmann and H. A. Makse, Rev. Mod. Phys., **90**, 015006 (2018).
  - [18] H.J. Herrmann and S. Luding, Continuum Mech. Thermodynamics, **10**, 189 (1998).
  - [19] A. Mehta, G. C. Barker and J. M. Luck, Proc. Natl. Acad. Sci. U.S.A., **105**, 8244 (2008).
  - [20] L. Atia, D. Bi, Y. Sharma, J. A. Mitchel, B. Gweon, S. A. Koehler, S. J. DeCamp, B. Lan, J. H. Kim, R. Hirsch, A. F. Pegoraro, K. H. Lee, J. R. Starr, D. A. Weitz, A. C. Martin, J.-A. Park, J. P. Butler and J. J. Fredberg, Nature Phys. **14**, 613 (2018).
  - [21] H. B. Callen and T. A. Welton, Phys. Rev., **83**, 34 (1951).
  - [22] R. Kubo, J. Phys. Soc. Japan, **12**, 570 (1957).
  - [23] J. Prost, J.-F. Joanny, and J. M. R. Parrondo, Phys. Rev. Lett., **103**, 090601, (2009).
  - [24] C. Maes, Phys. Rev. Lett., **125**, 208001 (2020).
  - [25] D. H. Wolpert, Phys. Rev. Lett., **125**, 200602, (2020).
  - [26] N. R. Morrow, Indust. Eng. Chem., **62**, 32 (1970).
  - [27] R. T. Armstrong and S. Berg, Phys. Rev. E, **88**, 043010, (2013).
  - [28] S. Berg, H. Ott, S.A. Klapp, A. Schwing, R. Neiteler, N. Brussee, A. Makurat, L. Leu, F. Enzmann, J. Schwarz, M. Kersten, S. Irvine, and M. Stamparoni, Proc. Natl. Acad. Sci. U.S.A., **110**, 3755, (2013).

- [29] R.T. Armstrong RT, H. Ott, A. Georgiadis, M. Rücker, A. Schwing and S. Berg, *Water Resour. Res.* **50** 9162 (2014).
- [30] L. Cueto-Felgueroso and R. Juanes, *Geophys. Res. Lett.* **43**, 1615 (2015)
- [31] N.R. Morrow, *Ind. Eng. Chem* **63**, 32 (1970).
- [32] S.M. Hassanizadeh and W.G. Gray, *Adv. Water Res.*, **16**, 53 (1993).
- [33] J. Bear and J.J. Nitao, *Transp. Porous Med.* **18**, 151 (1995).
- [34] C. Marle, “Multiphase Flow in Porous Media”, Editions Technip (1981).
- [35] S.A. Aryana and A.R. Kovscek, *Transp. Porous Med.* **97**, 373 (2013).
- [36] B. K. Primkulov, A.A. Pahlavan, X. Fu, B. Zhao, C.W. MacMinn and R. Juanes, *J. Fluid Mech.* **875**, R4 (2019).
- [37] A. A. Pahlavan, H. A. Stone, G. H. McKinley and R. Juanes. *Proc. Natl. Acad. Sci. U.S.A.* **116**, 13780 (2019).
- [38] H.B. Callen. *Thermodynamics*, (1960).
- [39] W.G. Gray and C.T. Miller, *Introduction to the Thermodynamically Constrained Averaging Theory for Porous Medium Systems*. Springer, Zürich, (2014).
- [40] S.R. De Groot and P. Mazur, *Non-Equilibrium Thermodynamics*, Dover (2013).
- [41] James Clerk Maxwell. *Theory of Heat*. Cambridge Library Collection - Physical Sciences. Cambridge University Press, 2011.
- [42] *Nature* 20, 126 (1879).
- [43] N. Shiraishi, Naoto and T. Sagawa, *Phys. Rev. E*, **91**, 012130 (2015).
- [44] J.V. Koski, V.F. Maisi, T. Sagava and J.P. Pekola, *Phys. Rev. Lett.* **113** 030601 (2014).
- [45] Hugo Touchette and S. Lloyd *Phys. Rev. Lett.* **84** 1156 (2000).
- [46] T. Sagawa and M. Ueda, *Phys. Rev. Lett.* **104** 090602. (2010).
- [47] E. Noether, *Gott. Nachr.*, **235**, 405 (1918).
- [48] E. Noether, *Transport Theory Stat. Phys.* **1**, 186 (1971).
- [49] J.D. Paulsen, R. Carmigniani, A. Kannan, J. C. Burton and S. R. Nagel, *Nat. Commun.*, **5**, 3182 (2014).
- [50] G. A. L. Dirk, H.N. Aarts, H.N. W. Lekkerkerker, H. Guo, G.H. Wegdam and D. Bonn, *Phys. Rev. Lett.*, **95**, 164503 (2005).
- [51] W. D. Ristenpart, P. M. McCalla, R. V. Roy and H. A. Stone, *Phys. Rev. Lett.*, **97**, 064501 (2006).
- [52] M. Wu, *Phys. Fluids.*, **16**, L51 (2004).
- [53] M. Orme, *Progress in Energy and Combustion Sci.*, **23** 65 (1997).
- [54] S. C. Case and S. R. Nagel, *Phys. Rev. Lett.*, **100**, 084503 (2008).
- [55] J.D. Paulsen, J.C. Burton and S.R. Nagel, *Phys. Rev. Lett.*, **106**, 114501 (2011).
- [56] J.D. Paulsen, J.C. Burton, S.R. Nagel, S. Appathurai, M.T. Harris and O.A. Basaran, *Proc. Natl. Acad. Sci. U.S.A.*, **109**, 6859 (2012).
- [57] S. Perumanath, M. K. Borg, M. V. Chubynsky, J. E. Sprittles and J. M. Reese, *Phys. Rev. Lett.*, **122**, 104501 (2019).
- [58] J. E. McClure, Z. Li, M. Berrill and T. Ramstad, *arXiv:2007.12266*, (2020).
- [59] M. B. Weissman, *Rev. Mod. Phys.* **60**, 537 (1988).
- [60] W.S. Kendal, *Physica A* **421**, 141 (2015).
- [61] P. Bak, C. Tang, and K. Wiesenfeld, *Phys. Rev. Lett.* **59**, 381 (1987).